We are IntechOpen, the world's leading publisher of Open Access books Built by scientists, for scientists

4,800
Open access books available

122,000
International authors and editors

135M
Downloads

Our authors are among the

154
Countries delivered to

TOP 1%
most cited scientists

12.2%
Contributors from top 500 universities

CLARIVATE ANALYTICS BOOK CITATION INDEX INDEXED

WEB OF SCIENCE™

Selection of our books indexed in the Book Citation Index in Web of Science™ Core Collection (BKCI)

Interested in publishing with us?
Contact book.department@intechopen.com

Numbers displayed above are based on latest data collected.
For more information visit www.intechopen.com

5

Elasticity of Spider Dragline Silks Viewed as Nematics: Yielding Induced by Isotropic-Nematic Phase Transition

Linying Cui[1], Fei Liu[2] and Zhong-can Ou-Yang[2]
[1]*Department of Physics, Tsinghua University, Beijing,*
[2]*Center for Advanced Study, Tsinghua University, Beijing,*
China

1. Introduction

Spider dragline silk (SDS), the main structural web silk regarded as the “spider’s lifeline", exhibits a fascinating combination of high tensile strength and high extensibility (1). Its toughness is over 10 times that of Kevlar, the material for making bullet-proof suits (2). In addition, SDS has a unconventional sigmoidal shaped stress-strain curve and shape memory capability after the tension and torsion test (3; 4) (Figure 1). All these intriguing properties have aroused the broad interest of scientists to understand the underlying deformation mechanism of SDS.

Leaving the open question of why SDS is that mechanically superb aside, people have already started to produce artificial SDS for numerous applications. Various methods to spin artificial SDS have been explored. These include conventional wet spinning of regenerated SDS obtained through forced silking (5; 6), solvent spinning of recombinant SDS protein analogue produced via bacteria and yeast cell cultures doped with chemically synthesized artificial genes (6; 7), and spinning of silk monofilaments from aqueous solution of recombinant SDS protein obtained by inserting the silk-producing genes into mammalian cells (6; 8). The applications also cover a broad biomedical range. For example, the silk-silica fusion proteins was used for bone regeneration by combining the self-assembling domains of SDS (*Nephila clavipes*) as scaffolds and the silaffin-derived R5 peptide of *Cylindrotheca fusiformis* that is responsible for silica mineralization (6; 9). Improved cell adhesion and proliferation of mouse osteoblast (MC3T3-E1) cells was achieved with films composed of *B. mori* fibroin and recombinantly produced proteins based upon *N. clavipes* SDS (incorporating the RGD integrin recognition sequence) *in vitro* (6; 10). SDS based antibacteria materials was also demonstrated by incorporating silk proteins with inorganic antibacteria nanoparticles such as silver nanoparticles (11) and titanium dioxide nanoparticles (12). In addition, silk films are promising candidates for biocompatible coatings for biomedical implants. For instance, gold nanoparticles, silver nanoparticles, and transition metal oxides/sulfides were dip-coated by SDS proteins and showed novel electrical, magnetic, optical properties, and at the same time, biocompatibility (6; 13–16).

Going back to the fundamental question of the structure-property relation of SDS, several experimental studies have been carried out to determine the supra-molecular structure of

SDS (17–22). X-ray diffraction patterns showed that there are many well oriented beta-sheet nanocrystals in the silk, with the long axis of the beta-sheet parallel to the silk axis (17–19). And polarized FTIR spectroscopy and Raman spectroscopy revealed more structures beyond the beta-sheet nanocrystal, including beta-coils, beta-turns, alpha-helices or the more compact and left-handed 3(1)-helices, all of which have quite low orientation in un-stressed SDS (1; 23–26). NMR data also suggested that there are two regions in SDS, a highly oriented beta-sheet nanocrystal region and a poorly oriented polypeptide chain region (22; 27; 28).Furthermore, these structural study results were confirmed by the protein sequence analysis (20; 29). Based on all these results, it is generally accepted that SDS is semicrystalline polymer with beta-sheet nanocrystals embedded in the amorphous region, which was a polypeptide chain network (23; 24; 30) (Figure 2(a)). The beta-sheet nanocrystals were always highly oriented to the axis of SDS, while the polypeptide chain network exhibited random orientation under zero external stress (19). When SDS was subjected to external tension stress, the orientation of the components in the polypeptide chain network was observed to increase significantly as the strain increased (17; 25; 28).

A few models were proposed (18; 23; 30; 31) to understand the structure-property relation of SDS based upon deformation theories of polymers and composite materials. For example, the model by Termonia (23) treated SDS as a hydrogen-bonded amorphous matrix embedded with stiff crystals as cross-links. In the interfacial region, an extremely high modulus is required to get SDS's overall behavior on deformation. While in the model of Porter and Vollrath (30; 31), parameters linking to chemical compositions and morphological order were used to interpret thermo-mechanical properties of SDS. But some parameters such as ordered/disordered fractions are difficult to be obtained from experiments. A recent model (18) connecting deformations on the macroscopic and molecular length scales still did not consider the change of the orientation of nanocomposites during deformation. Especially, as pointed out by Vehoff *at al.* recently (32), basic polymer theories such as the freely jointed chain, the freely rotating chain and the worm-like chain, as well as a hierarchical chain model of the spider capture silk (33) could not reproduce the sigmoidal shape or even the steep initial regime of SDS (Fig. 2(a)) (32). While nonlinear polymer theories can give a general description of the entire deformation process of the silk, some special conditions are invoked (30; 31) and the uniqueness in SDS is not taken into account. In one word, a more natural and unified description for the extraordinary properties of SDS as a model biomaterial still seems to be lacking.

Quite a few works (4; 17; 19; 22; 34–37) have pointed out that SDS is liquid crystalline material and liquid crystal (LC) phase plays a vital role in both its spinning process and mechanical properties. In the spinning process, the spider's 'spinning dope' is liquid crystalline, which make it possible to efficiently spin a thread from large silk protein molecules (4; 38–40). Specifically, in the spider's gland and duct the molecules form a nematic phase (4; 38) — a phase that makes the silk solution flow as a liquid but maintain some of the orientational order characteristic of a crystal, with the long axes of neighboring molecules aligned approximately parallel to one another. In the final extrusion stage of the spinning process, the liquid crystal phase is even more enhanced and frozen into the beta-sheet structure of the silk: The forming thread stretches, narrows and pulls away from the walls of the duct, which bring the dope molecules into better alignment and into a more extended conformation to facilitate hydrogen bonds formation to give the anti-parallel beta conformation of the final thread (4; 38). The final silk contains 40 vol % anti-parallel beta-nanocrystals highly aligned to the silk axis as a frozen LC phase from the spinning process (31).

For the solid SDS, the LC phase transition is an important feature in SDS's deformation process and contributes a lot to the silk's combination of high strength and high extensibility, as well as the shape memory property. In the unstressed state of SDS, the polypeptide chain network has random orientation (25) with many components present, such as beta-coils, beta-turns, alpha-helices or the more compact and left-handed 3(1)-helices (1; 22–24; 26). All of these structures have elongated shapes and the tendency to form LC phase (41). Under increasing tensile stress, the orientations of the elongated components increase substantially as revealed by polarized FTIR spectroscopy and DECODER (direction exchange with correlation for orientation distribution evaluation and reconstruction) NMR (25; 28). The sigmoidal shape of the stress-strain curve (Figure 1(a)) indicates that a LC phase transition takes place at the yield point, resulting in the huge extensibility of SDS after the yield point.
Although some work proposed SDS to be a biological LC elastomer together with the silkworm's silk (37), a detailed description of the deformation mechanism of SDS from the LC point of view is lacking. We constructed an analytical LC model. The polypeptide chain network is set to be in the isotropic state at the beginning with the tendency to transit into the LC phase. Under external stress, the Maier-Saupe theory (42) of nematic LC is employed to monitor the change of the orientation of the polypeptide chain network. We show that during deformation SDS undergoes significant increase of the orientation of the chain network, with a force-induced isotropic-nematic phase transition at the yield point which especially facilitates the extension of the SDS after the yield point. The comprehensive agreement between theory and experiments on the stress-strain curve strongly indicates SDS to belong to LC materials. Especially, the remarkable yielding elasticity of SDS is understood for the first time as the force-induced isotropic-nematic phase transition of the chain network. The present theory also predicts a drop of the stress in supercontracted SDS, an early found effect of humidity on the mechanical properties in many silks (30; 32; 43).

2. Model

Because the beta-sheet nanocrystal has high orientation along the silk axis as spun and deforms much smaller than that of the bulk (17), we will neglect the deformation and rotation of the beta-sheet nanocrystal under external stress and focus on the deformation change of the amorphous polypeptide chain network in the current work. This assumption is also supported by the observations that SDS's high extensibility results primarily from the disordered region (18; 20; 21), and that the deformation of the beta-sheet nanocrystal is at least a factor of 10 smaller than that of the bulk (17).
We take the polypeptide chain network in the amorphous region of SDS as a molecular LC field with each chain section corresponding to a mesogenic molecule (i.e. a molecule having the tendency to form liquid crystal phase under specific conditions); see Fig. 2. Following the LC continuum theory in the absence of forces, the potential of a mesogenic molecule takes the Maier-Saupe interaction form (42)

$$V(\cos\theta) = -aS(\frac{3}{2}\cos^2\theta - \frac{1}{2}), \tag{1}$$

where θ is the angle between the long axis of the molecule and the silk axis (the z-axis), which is also the direction of $\hat{\mathbf{n}}$ (Fig. 2 (b)). a is the strength of the mean field. S is the orientation

order parameter of the LC, defined as the average of second Legendre polynomial (41)

$$S = \left\langle \frac{3}{2}\cos^2\theta - \frac{1}{2} \right\rangle. \tag{2}$$

We notice that the Maier-Saupe potential has been used by Pincus and de Gennes when investigating LC phase transition in a polypeptide solution (44). Using the LC potential to describe the interaction between the segments of the polypeptide chain network is a good mean-field approach because a large part of the polypeptide chain network bears alpha helix and beta coil structures (20; 24), which tend to form a LC phase due to their elongated shape (41). When a uniform force field **f** along z-axis is applied, the potential of a molecule is written as

$$U(\cos\theta) = V - fl\cos\theta, \tag{3}$$

where l denotes the length of the mesogenic molecule.
From the definition of the order parameter S, we get a self-consistency equation

$$\begin{aligned} S = {} & \textstyle\int_{-1}^{1} (\frac{3}{2}\cos^2\theta - \frac{1}{2}) \exp(\frac{3aS}{2k_BT}\cos^2\theta + \alpha\cos\theta) d\cos\theta \\ & \Big/ \textstyle\int_{-1}^{1} \exp(\frac{3aS}{2k_BT}\cos^2\theta + \alpha\cos\theta) d\cos\theta \ , \end{aligned} \tag{4}$$

with $\alpha = fl/k_BT$. The solution of the above equation may not be unique, in order to obtain physically sound solution we need to apply the free energy minimization criterion (41) given by

$$F_{MS} = -k_BT\ln Z + \frac{1}{2}aS^2, \tag{5}$$

where Z is the partition function $Z = \int_{-1}^{1} e^{-U(\cos\theta)/k_BT} d\cos\theta$, and the second term at the right-hand side corrects for the double counting arising from the mean field method (45).
The orientation function S was calculated numerically at different temperatures $T^* = T/T_{ni}$ and forces f, and the results were shown in Fig. 3(b). Here $T_{ni} = a/(4.541k_B)$ is the isotropic-nematic transition temperature in the absence of forces (42). At temperatures below T_{ni} the molecules have spontaneous nematic order, and the force does not induce further order significantly. While for the molecules initially in paranematic state (i.e. an isotropic state close to the nematic state), the applied force field will induce a first-order phase transition — S jumps discontinuously to a higher value at a certain critical force $f_C(T^*)$. At even higher temperatures, nematic field is weaker and the effect of the force is less dramatic.
To compare with experiment data, we give the expressions of stress and strain in our model. Apparently, the stress σ of the bulk is $\sigma \equiv F/A = Nf$: F is the force on the surface of the bulk, A is the area of the surface, and N is the number of molecules per area. The strain ε of the bulk is defined as $\varepsilon = [L(f) - L_0]/L_0$, where $L(f)$ is the length of the bulk along z-axis when the force field **f** is applied and we can take it as $L(f) = \langle l|\cos\theta|\rangle$, and $L_0 = L(f=0) = l/2$. Then the strain ε is $\varepsilon = 2\langle|\cos\theta|\rangle - 1$. The curve of ε versus σ at different temperatures is shown in Fig. 3(c). At temperatures below T_{ni}, the strain grows smoothly with the stress. For temperatures just above T_{ni}, the strain grows with the stress in an almost linear way under small forces, then a jump in the strain occurs at the critical force $f_C(T^*)$, after which the strain increases smoothly with the stress again. At higher temperatures, the nematic field is weaker

and the jump is replaced by a smooth increase in strain, with a plateau in a certain range of force.

In our model, the reduced temperature T^* is an essential parameter, which needs to be chosen specifically in order to predict the stress-strain curve of SDS. Because the silk solution is in LC state at ambient temperature (4; 34; 35) while for the solid silk the orientation of the polypeptide chain network is very low (25), it is likely that the solid polypeptide chain network still has a high tendency to form LC state and is in paranematic state under zero loading. Namely, the isotropic-nematic transition temperature $T_{\rm ni}$ of the chain network is slightly lower than the room temperature T_r, i. e. T^* is just above 1. Actually, the curves of $T^* = 1.01$ and 1.02 agree well with the experimental stress-strain curve of SDS, with a steep linear relation at the beginning and more abrupt increase of the strain after the yield point. Due to viscoelasticity (46), defects and polydomain effects (45), the real SDS exhibit a smoother strain increase after the yield point, while the non-viscoelastic and defect-free LC model predicts an abrupt increase of the strain. From the curves of $T^* = 1.01$ and 1.02, we get the estimation of the yield strain $\varepsilon_y \approx 0.04$, the yield stress $\sigma_y = \alpha N {\rm k_B} T/l \approx 8.4$MPa, and the Young's modulus at the linear region $E \equiv \sigma_y/\varepsilon_y \approx 210$MPa, given $\alpha \sim 0.2$, $N/l \sim 10{\rm nm}^{-3}$, and ${\rm k_B}T_r \sim 4.1$pNnm. These estimations well agree with the experimental results for the low reeling speed SDS, with the yield strain $\varepsilon_y \approx 0.04$, the yield stress $\sigma_y \approx 10$MPa, and the Young's modulus at the linear region $E \approx 250$MPa (Fig. 3(d)) (19).

3. Discussion

The stress-strain curve of paranematic state in the LC model well explains the main features of the stress-strain curve of SDS: With low loading, entropy is dominating and the polypeptide chain network is isotropic. Mesogenic molecules only respond individually to the external stress field by rotating a little bit to the stress direction on average, so the increase of the strain is small and the Young's modulus is high. As the stress increases, the competition between the entropy and the mesogenic molecule potential (including the LC field and the external force field) in the free energy expression (Eq. 3 and 5) begins to favor the potential field. At the point when the potential begins to dominate over the entropy, the isotropic-nematic phase transition of the mesogenic molecule network (i.e. the polypeptide chain network) occurs. Mesogenic molecules start to rotate collectively to the stress direction to form the nematic LC phase. Since all components in the polypeptide chain network tend to align parallel to the silk axis, the length of the silk increases substantially under a constant stress, resulting in the plateau following the transition initiation point which is called the yield point. Due to viscoelasticity (46), defects and polydomain effects (45), the real SDS has a smoother plateau in the stress-strain curve with the same fact that the majority of the SDS's extensibility results from the softening plateau after the yield point. When the stress increases further, the orientation of the network grows rapidly, as observed by polarized FTIR spectroscopy and DECODER (direction exchange with correlation for orientation distribution evaluation and reconstruction) NMR (25; 28). Finally, the shape memory property of SDS in the tension test can be understood as a reverse phase transition process when the external stress decreases to zero.

In the LC model, we predict an isotropic-nematic phase transition at the yield point. Several experimental observations do support a significant increase of the orientation of the elongated components in the amorphous region with various strain. For example, a polarized FTIR spectroscopy measurement (25) showed that the orientation of some components in the

amorphous region increased by 0.3 when the strain reached 24%. A NMR study also suggested the alignment of the components in the amorphous region became poor in the strain relaxation process (28). Further experimental work needs be done to track the orientation change of the polypeptide chain network in the deformation process of SDS in order to better understand its LC character.

We notice that our results agree much better with the mechanical properties of the silks produced by low reeling speed. That is because a high reeling speed will induce a low orientation in the amorphous region, which is not taken into account in the current work.

In addition to describing the stress-strain relation of SDS, our LC model can also qualitatively account for the drop of the stress in wet SDS, *i.e.* the supercontracted SDS. Take L_0 and R_0 as the initial length and radius of the silk, and L and R as those under stress. Under the assumption of volume conservation we have $\pi R_0^2 L_0 = \pi R^2 L$, so $R/R_0 = \sqrt{1/(1+\varepsilon)}$. The free energy of the bulk can be written as

$$\begin{aligned} F &= V - f_{ext}(L - L_0) + 2\pi R L\gamma \\ &= V - f_{ext}(L - L_0) + 2\pi R_0 L_0 \gamma\sqrt{1+\varepsilon}, \end{aligned} \tag{6}$$

where V is the internal energy of the bulk, f_{ext} is the external force on the bulk and γ is the surface energy coefficient. Minimizing F with respect to ε, we get

$$\sigma = \frac{f_{ext}}{\pi R_0^2} = \frac{1}{\pi R_0^2 L_0}\frac{\partial V}{\partial \varepsilon} + \frac{\gamma}{R_0\sqrt{1+\varepsilon}}. \tag{7}$$

When the silk is immersed in water, the surface energy coefficient γ increases, so with the same stress σ we need a bigger strain. Thus our theory can predict the softening of supercontracted silk, an effect observed in many experiments (30; 32; 43; 47; 48).

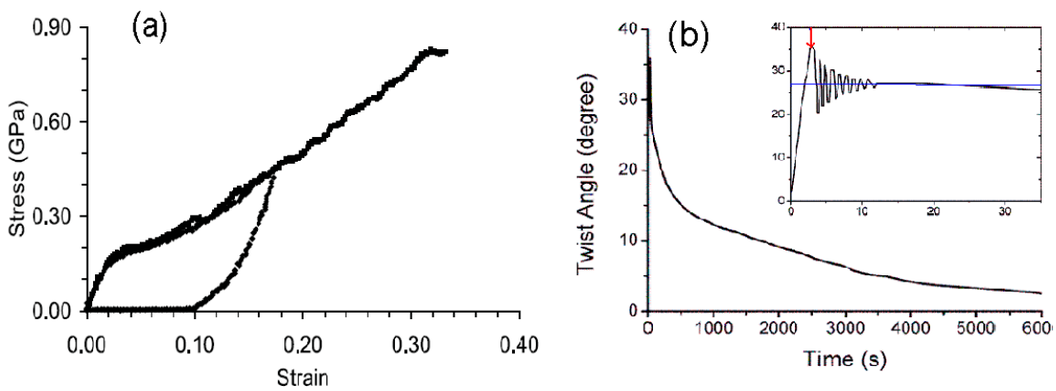

Fig. 1. (a). The stress-strain curves of a spider silk in a deformation cycle and during strain to break. (31) (b). Relaxation dynamics of a torsion pendulum for a spider silk thread. Inset: zoom of the start of the self-relaxation dynamics. The red arrow indicates the end of the excitation and the start of the free relaxation period. Blue line, new equilibrium position. (3)

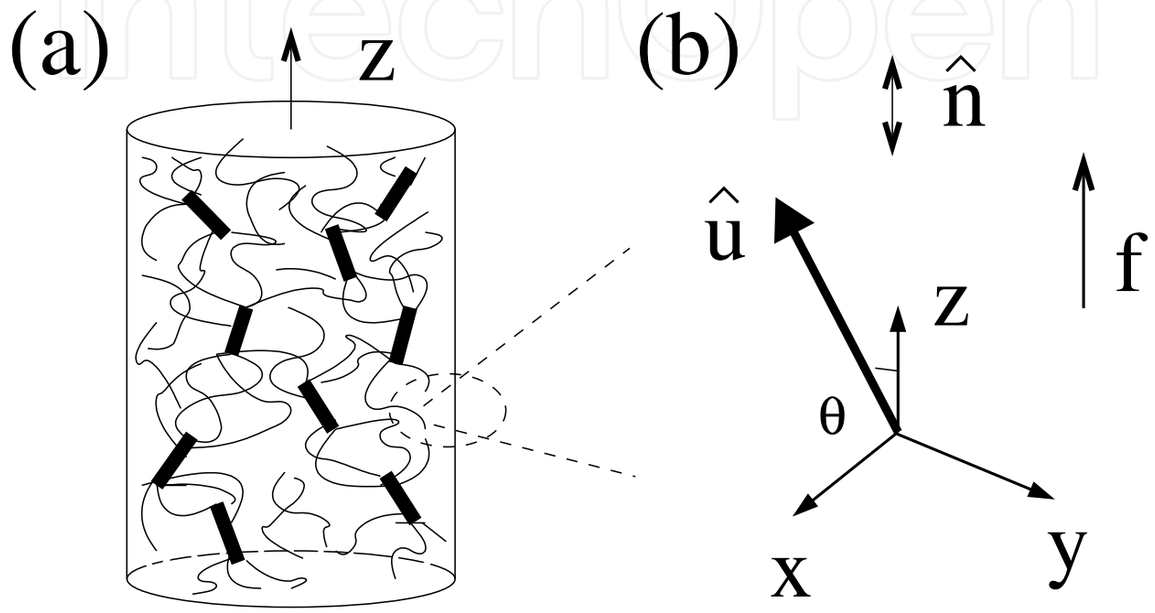

Fig. 2. (a). A schematic diagram of the structure of the dragline silk. The bold lines represent the β-sheet crystals, and the thin lines represent the polypeptide chains in the amorphous region. The z-axis is along the silk axis. (b). The coordinate system of the nematics. $\hat{\mathbf{n}}$ is the director of the nematics, $\hat{\mathbf{u}}$ is the director of the mesogenic molecule, and θ is the angle between the long axis of the molecule and the silk axis z.

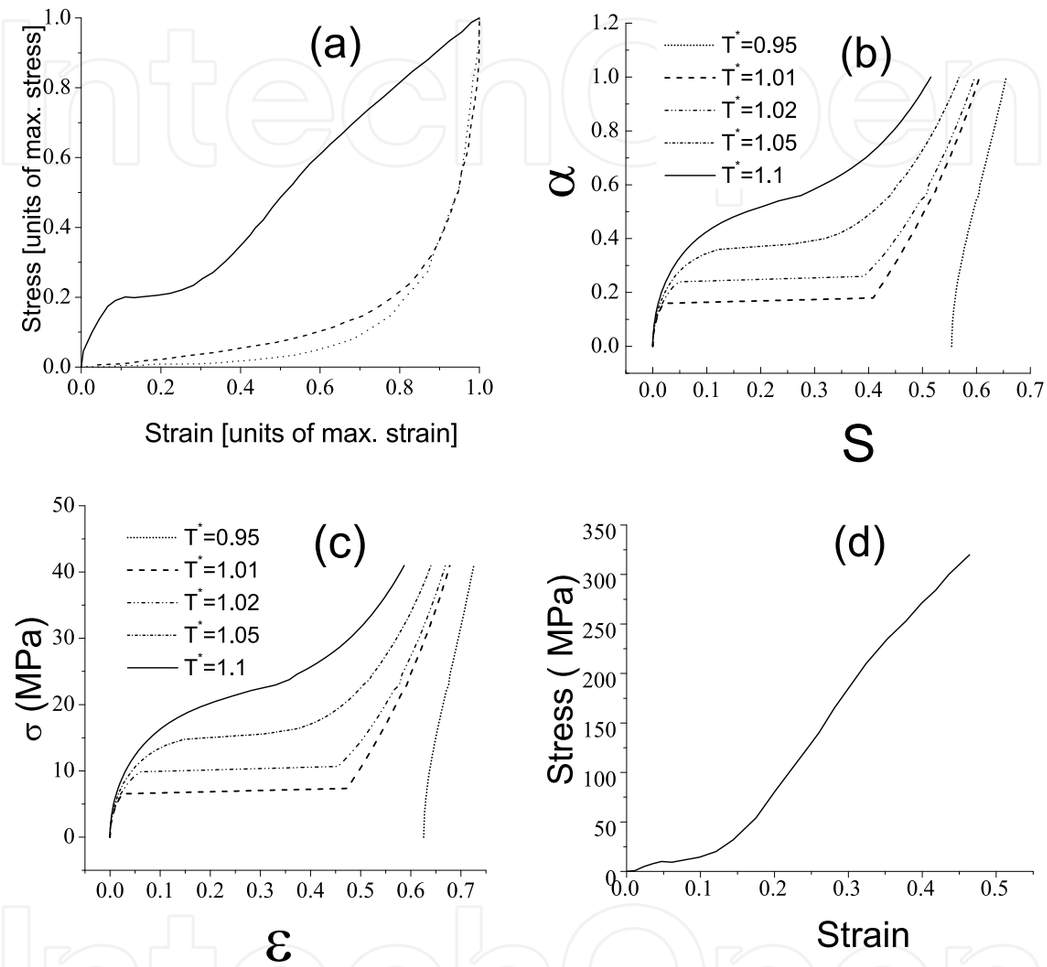

Fig. 3. (Color online.) (a) Comparison of a typical measured dragline silk's stress-strain curve (black solid line) with theoretical curves evaluated by the freely jointed chain (red dash dot line) and the hierarchical chain model (olive dash line) [After T. Vehoff *et al.*]. (b) The orientation order parameter S as a function of $\alpha(= fl/\mathrm{k_B}T)$. (c) The stress-strain curves at different temperatures $T^*(= T/T_{\mathrm{ni}})$. Calculated with $N/l \sim 10\mathrm{nm}^{-3}$, and $\mathrm{k_B}T_r \sim 4.1\mathrm{pNnm}$. (d) The stress-strain curve of the SDS spinned with the speed of $1\mathrm{mms}^{-1}$ (19).

4. Conclusion

In conclusion, we investigate the mechanical properties of SDS from the view point of LC continuum theory. This LC approach is justified by the following considerations: 1) Solid SDS is spined from a polypeptide LC solution and has well aligned beta-sheet nanocrystals as a frozen-in LC phase (36). 2) A large part of the amorphous region (the polypeptide chain network) of the solid SDS has alpha-helix and beta-coils secondary structures, which tend to form LC phase due to their elongated shape (41). 3) By solving a self-consistent equation, both the stress-strain relation and the orientation-reduced temperature relation are obtained from the LC model. These curves agree well with the experimental curves quantitatively and especially help to interpret the high extensibility behavior of SDS at the yield point. 4) The LC model can also describe the shape memory and the supercontraction properties of SDS. 5) The major energy term, the Maier-Saupe potential (41), in the LC model shares the same physical background with the essential energy contributor, the cohesive energy, in polymer theory (31; 49). They both origin from van der Waals forces, although with different emphasis: The LC model focuses on understanding the orientation change and the contribution of LC phase transition to the high extensibility of SDS; while the conventional polymer theories emphasize on either phenomenological descriptions (18) or molecular modelings with high computation requirements (31).
Ongoing work is to develop the model to understand more of the fascinating properties of SDS. More experimental work is highly needed as well to further verify the LC model.

5. References

[1] J. M. Gosline, M. W. Denny, and M. E. Demont, Nature **309**, 551 (1984).
[2] I. Agnarsson, M. Kuntner, T. A. Blackledge, PLoS ONE**5**, e11234 (2010).
[3] O. Emile, A. L. Floch, and F. Vollrath, Nature **440**, 621 (2006).
[4] F. Vollrath and D. P. Knight, Nature **410**, 541 (2001).
[5] M. Kang M, and H. J. Jin, Colloid. Polym. Sci.**285**, 1163 (2007).
[6] J. G. Hardy, and T. R. Scheibel, Prog. Polym. Sci.**35**, 1093 (2010).
[7] C. Fu, Z. Shao, F. Vollrath, Chem. Mater., 6515 (2009).
[8] H. Kim *et al.*, J. Nanosci. Nanotechnol.**8**, 5543 (2008).
[9] A. J. Mieszawska *et al.*, Chem. Mater.**22**, 5780 (2010).
[10] A. W. Morgan *et al.*, Biomaterials**29**, 2556 (2008).
[11] M. Kang *et al.*, J. Nanosci. Nanotechnol.**7**, 3888 (2007).
[12] Y. Xia, G. Gao, and Y. Li, J. Biomed. Mater. Res. Part B**90**, 653 (2009).
[13] A. Singh, S. Hede, and M. Sastry, Small**3**, 466 (2007).
[14] Y. Zhou *et al.*, Chem. Commun.**23**, 2518 (2001).
[15] N. Kukreja *et al.*, Pharmacol Res**57**, 171 (2008).
[16] H. S. Yin, S. Y. Ai, W. J. Shi, and L. S. Zhu, Sens. Actuators B**137**, 747 (2009).
[17] A. Glisąęovic, T. Vehoff, R. J. Davies, and T. Salditt, Macromolecules **41**, 390 (2008).
[18] I. Krasnov *et al.*, Phys. Rev. Lett. **100**, 048104 (2008).
[19] N. Du *et al.*, Biophys. J. **91**, 4528 (2006).
[20] C. Y. Hayashi and R. V. Lewis, J. Mol. Biol. **275**, 773 (1998).
[21] E. Oroudjev *et al.*, Proc. Natl. Acad. Sci. USA **99**, 6460 (2002).
[22] A. H. Simmons, C. A. Michal, and L. W. Jelinski, Science **271**, 84 (1996).
[23] Y. Termonia, Macromolecules **27**, 7378 (1994).

[24] T. Lefevre, M. E. Rousseau, and M. Pezolet, Biophys. J. **92**, 2885 (2007).
[25] P. Papadopoulos, J. Solter, and F. Kremer, Eur. Phys. J. E **24**, 193 (2007).
[26] J. Kummerlen *et al.*, Macromolecules **29**, 2920 (1996).
[27] J. Beek *et al.*, Proc. Natl. Acad. Sci. USA **99**, 10266 (2002).
[28] P. T. Eles and C. A. Michal, Biomacromolecules **5**, 661 (2004).
[29] M. Xu, and R. V. Lewis, Proc. Natl. Acad. Sci. USA **87**, 7120 (1990).
[30] F. Vollrath and D. Porter, Soft Matter **2**, 377 (2006).
[31] D. Porter, F. Vollrath, and Z. Shao, Eur. Phys. J. E **16**, 199 (2005).
[32] T. Vehoff, A. Gliąęsoviąäc, H. Schollmeyer, A. Zippelius, and T. Salditt, Biophys. J. **93**, 4425 (2007).
[33] H. J. Zhou and Y. Zhang, Phys. Rev. Lett. **94**, 028104 (2005).
[34] K. Kerkam, C. Viney, D. Kaplan, and S. Lombardi, Nature **349**, 596 (1991).
[35] P. J. Willcox, S. P. Gido, W. Muller, and D. L. Kaplan, Macromolecules **29**, 5106 (1996).
[36] E. T. Samulski, Liquid Crystalline Order in Polymers, edited by A. Blumstein, (Academic Press, New York, 1978), Chap. 5, p. 186.
[37] D. P. Knight and F. Vollrath, Phil. Trans. R. Soc. Lond. B **357**, 155 (2002).
[38] D. Knight and F. Vollrath, Proc. R. Soc. Lond. B **266**, 519 (1996).
[39] K. Kerkam *et al.*, Nature **349**, 596 (1991).
[40] P. J. Wilcox *et al.*, Macromolecules **29**, 5106 (1996).
[41] P. G. de Gennes, J. Prost, The Physics of Liquid Crystals(2nd edt), (Clarendon Press, Oxford, 1993).
[42] W. Maier and A. Saupe, Z. Naturforsch. A., 14, 882 (1959).
[43] F. I. Bell, I. J. McEwen, and C. Viney, Nature **416**, 37 (2002).
[44] P. Pincus and P. G. de Gennes, J. Polymer Sciences: Polymer Symposium **65**, 85 (1978).
[45] M. Warner, E. M. Terentjev, Liquid Crystal Elastomers, (Clarendon Press, Oxford, 2003).
[46] R. W. Work, J. exp. Biol. **118**, 379 (1985).
[47] R. W. Work, Textile Res. J. **47**, 650 (1977).
[48] R. W. Work, J. Arachnol. **9**, 299 (1981).
[49] D. Porter, Group Interaction Modelling og Polymer Properties, (Marcel Dekker, New York, 1995).

Biomaterials Applications for Nanomedicine

Edited by Prof. Rosario Pignatello

ISBN 978-953-307-661-4
Hard cover, 458 pages
Publisher InTech
Published online 16, November, 2011
Published in print edition November, 2011

These contribution books collect reviews and original articles from eminent experts working in the interdisciplinary arena of biomaterial development and use. From their direct and recent experience, the readers can achieve a wide vision on the new and ongoing potentialities of different synthetic and engineered biomaterials. Contributions were selected not based on a direct market or clinical interest, but on results coming from a very fundamental studies. This too will allow to gain a more general view of what and how the various biomaterials can do and work for, along with the methodologies necessary to design, develop and characterize them, without the restrictions necessary imposed by industrial or profit concerns. Biomaterial constructs and supramolecular assemblies have been studied, for example, as drug and protein carriers, tissue scaffolds, or to manage the interactions between artificial devices and the body. In this volume of the biomaterial series have been gathered in particular reviews and papers focusing on the application of new and known macromolecular compounds to nanotechnology and nanomedicine, along with their chemical and mechanical engineering aimed to fit specific biomedical purposes.

How to reference

In order to correctly reference this scholarly work, feel free to copy and paste the following:

Linying Cui, Fei Liu and Zhong-Can Ou-Yang (2011). Elasticity of Spider Dragline Silks Viewed as Nematics: Yielding Induced by Isotropic-Nematic Phase Transition, Biomaterials Applications for Nanomedicine, Prof. Rosario Pignatello (Ed.), ISBN: 978-953-307-661-4, InTech, Available from: http://www.intechopen.com/books/biomaterials-applications-for-nanomedicine/elasticity-of-spider-dragline-silks-viewed-as-nematics-yielding-induced-by-isotropic-nematic-phase-t

INTECH
open science | open minds

InTech Europe
University Campus STeP Ri
Slavka Krautzeka 83/A
51000 Rijeka, Croatia
Phone: +385 (51) 770 447
Fax: +385 (51) 686 166
www.intechopen.com

InTech China
Unit 405, Office Block, Hotel Equatorial Shanghai
No.65, Yan An Road (West), Shanghai, 200040, China
中国上海市延安西路65号上海国际贵都大饭店办公楼405单元
Phone: +86-21-62489820
Fax: +86-21-62489821

IntechOpen